Process Simulation and Retrofit Optimisation for Cleaner-Fuel Naphtha Distillation

I&EC research
Industrial & Engineering Chemistry Research

pubs.acs.org/IECR
Article

Process Simulation and Retrofit Optimization for Cleaner-Fuel Naphtha Distillation

Pedro Dias, Abbas Rajaei, and Nejat Rahmanian*

Cite This: *Ind. Eng. Chem. Res.* 2025, 64, 23622−23637

ABSTRACT: This study presents a digital-twin case analysis of a South African refinery's naphtha splitter, integrating Aspen HYSYS V12 simulation with the plant data. The objective was to balance energy efficiency with benzene control under Clean Fuels II (CF2) regulations. The Aspen HYSYS model, validated against plant data with mean absolute percentage deviations of ≈10% for light- and 14% for heavy-naphtha compositions, was used to identify two successive optimization pathways. First, tuning existing operational variables achieved a 14% reduction in total energy duty, corresponding to about US $1.4 million in annual savings, with zero capital modification. Second, introducing a low-CAPEX midcolumn side-draw to remove benzene-forming precursors further improved performance, delivering a total energy reduction of ≈33% relative to the original baseline. Together, these measures demonstrate how an existing splitter can be retrofitted for lower emissions and cleaner-fuel production. The methodology, plant-calibrated analysis coupled with staged operational and structural optimization, provides a transferable framework for energy-intensive distillation units around the globe seeking rapid, economical decarbonization.

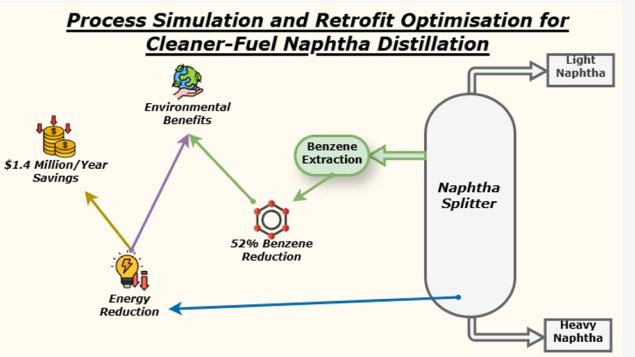

1. INTRODUCTION

South Africa's refining sector is dominated by a handful of operators that supply both national and regional fuel demand.[1] Within these facilities, the naphtha splitter plays a vital role in separating whole naphtha into light and heavy fractions. Light naphtha is directed to isomerization units to improve octane through branching, while heavy naphtha is routed to catalytic reformers to generate high-octane aromatics for gasoline blending.[2] The splitter's performance, therefore, has a direct influence on product quality, energy efficiency, and compliance with emerging fuel regulations.

These pressures are intensifying under Clean Fuels II (CF2) specifications, which mandate that benzene in gasoline be reduced from 5 vol % to ≤1 vol % by July 2027; local refiners are already executing compliance programs in response.[3,4] At the same time, energy remains the dominant share of refinery OPEX: DOE/ENERGY STAR reports indicate that 30−50% of refinery cash operating costs are energy-related,[5] while distillation columns alone can consume more than one-third of this energy.[6] This combination of rising environmental standards and cost exposure underscores the strategic importance of revamping existing separation assets before turning to capital-intensive unit replacements.

Several approaches to splitter optimization have been reported in the literature. Work on heat-integrated distillation columns (HIDiC) and dividing-wall columns (DWCs) has demonstrated substantial efficiency and debottlenecking potential.[7−9] DWCs in particular have been applied in naphtha service, enabling simultaneous improvement in cut quality and energy intensity, though they demand significant modifications and capital investment.[6] In parallel, simulation-based case studies show that benzene and aromatic removal can be improved via side cuts and column sequencing, with studies in catalytic-cracking gasoline demonstrating meaningful benzene reduction when column configurations and operating policies are optimized.[10] Similarly, recent work on naphtha recycle isomerization units has shown that column modifications such as the addition of a deisopentanizer can substantially improve product quality and compliance with fuel norms.[11] However, most of these works treat energy efficiency and aromatic control separately, overlooking their combined impact.

From a design perspective, side-draws remain an attractive low-CAPEX tool: the composition of a side stream equals that of the tray liquid where it is taken, meaning draw location directly determines cut quality and introduces an additional control degree of freedom.[12,13] Such modifications are particularly relevant when considering benzene precursors such as methyl cyclopentane and cyclohexane, which readily convert to benzene

Received: August 13, 2025
Revised: November 16, 2025
Accepted: November 18, 2025
Published: November 26, 2025

https://doi.org/10.1021/acs.iecr.5c03368
Ind. Eng. Chem. Res. 2025, 64, 23622−23637

during reforming.[14,15] Selective removal of these species upstream can mitigate benzene formation in the reformer, offering both compliance and product-quality benefits.

Simulation tools provide the framework for evaluating these strategies. The Peng−Robinson (PR) equation of state is widely used for C5−C10 hydrocarbon mixtures, balancing simplicity with robust vapor−liquid equilibrium predictions.[11,16,17] Recent refinery optimization studies further highlight the value of simulation-based revamp design, from operating policy adjustments[18] to column configuration changes.[11] These works show that leveraging simulation allows refiners to extract more value from existing assets before committing to high-CAPEX upgrades.

In this context, the present study contributes an industrial case analysis of a South African refinery's naphtha splitter. We combine Aspen HYSYS simulation with plant data validation to explore operating levers—feed pressure, feed temperature, reflux ratio—and introduce a side-draw configuration aimed at benzene reduction. The study addresses a critical gap in the literature by jointly considering energy efficiency and benzene compliance under real-world constraints, demonstrating how low-cost operational strategies can deliver rapid savings and regulatory readiness while deferring major capital investment.

2. METHODOLOGIES

This study followed a structured methodology, shown in Figure 1, similar to other real-world case studies, such as Rahmanian et al.[19] and Rahmanian et al.,[20] beginning with data gathering at the refinery, followed by the development of the base case HYSYS model and its validation. A sensitivity analysis on the key process conditions was conducted to identify optimal operating points. After an optimized short-term operating point was achieved, a new configuration was simulated and further analyzed, focusing on benzene removal. This process concluded with the insights and recommendations explored from comparing the base and improved models.

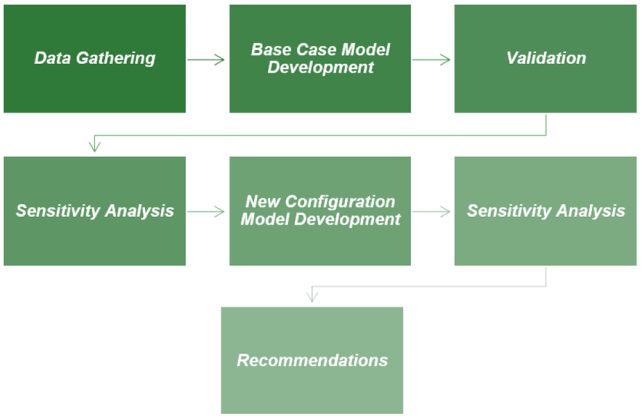

Figure 1. Flowchart of the methodology used in this study.

2.1. Data Collection and Analysis. The first step in this study was to gather data from the plant, as this formed the foundation for the development of the simulation and validation.

Operational data for a determined 15-day period of stable operation was collected by the authors from the plant using a combination of sources, including the Distributed Control System (DCS), PI Datalink, and outlet samples. Pressure, temperature, reflux ratios, flow rates and energy consumption parameters were recorded for this period. While this span ensured consistency, it only represents the normal operating conditions rather than the full range of refinery variations, such as feedstock shifts and operating upsets, tray flooding or equipment malfunction. Quality control was vital to ensure data reliability. Therefore, the initial data sets were cross-referenced across various sources, and any discrepancies identified during this stage were reconciled with plant engineers to ensure consistency between simulation inputs and actual plant data.

2.2. Base Case Development. After defining the feed composition, shown in Table 1, an appropriate fluid package had to be selected to ensure that the simulation accurately captured the relevant phase behavior and property correlations.

Table 1. Feed Composition after the Control Valve

Components	LiqVol Fractions
Benzene	0.0108
i-Butane	0.0010
n-Butane	0.0441
Cyclopentane	0.0076
i-Pentane	0.0631
n-Pentane	0.0715
Cyclohexane	0.0001
Mcyclopentane	0.0085
2-Mpentane	0.0404
22-Mbutane	0.0068
23-Mbutane	0.0068
3-Mpentane	0.0255
n-Hexane	0.0490
Toluene	0.0310
11Mcyclopentane	0.0595
Mcyclohexane	0.1280
2-Mhexane	0.0507
n-Heptane	0.0479
E-Benzene	0.0362
1-ci2-MCC6	0.0971
n-Octane	0.0348
124-MBenzene	0.0108
1c3c5MCC6	0.0513
n-Nonane	0.0191
12-E-BZ	0.0003
11-Di-E-CC6	0.0062
n-Decane	0.0018
2244Mpentane	0.0154
224-Mpentane	0.0435
225-Mhexane	0.0310

In addition to its widespread industry acceptance, the Peng−Robinson Equation of State (EOS) was chosen as it provides a good balance between complexity and applicability for predicting hydrocarbon mixtures—a key requirement for this simulation.[16,17]

In the simulation environment, the first step was to characterize the feed based on sample and operational data, including volumetric flow rates, temperature, pressure, and volumetric fractions for each component as seen below. It is important to note that available data corresponded to feed conditions before the pressure drops across the control valve, which was replicated in Aspen HYSYS to reflect actual process behavior.

The simulation was then initiated by mapping out the entire process flow of the Naphtha Splitter, identifying all process

https://doi.org/10.1021/acs.iecr.5c03368
Ind. Eng. Chem. Res. 2025, 64, 23622−23637

streams and key equipment of the system and stream compositions, as demonstrated below in Figure 2.

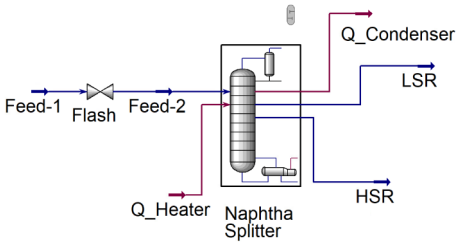

Figure 2. Base case Aspen HYSYS model.

Once all necessary inputs were fully specified—including feed properties, column internals, and configuration—the initial simulation was run, aiming to replicate the operational profiles observed in the actual plant. Although the initial simulation generated minor deviations in product compositions and flow rates, these preliminary outputs provided a solid foundation for further analysis. There was an emphasis on comparing the product compositions and matching them directly with plant measurements, with any variances described in the next sections. This calibration process was conducted by adjusting tray efficiencies (set to 80%) and tuning other monitored column parameters until a close match was achieved between the simulation and real plant data.

2.3. Sensitivity Analysis. This sensitivity analysis was designed to assess the impact of varying process conditions and column parameters, such as pressure, temperature, and reflux ratio, on the performance of the column. This assisted in determining which variables influence product quality and energy consumption the most, the trade-offs between separation and energy efficiency and ultimately identifying the optimal operating range for the column. This analysis will ultimately serve as a foundational step for future multiobjective optimizations.

For each parameter, various simulation runs were made while keeping all other variables constant, which allowed for a better understanding of each parameter's contribution to the system. Feed temperature was varied from 110 to 140 °C, while pressure was varied from 140 to 300 kPa; these operating ranges were selected to reflect both the operating limits of the existing equipment. At the same time, the reflux ratio was varied between 1.5 and 6, which encompasses the normal operating point.

This sensitivity analysis generated a set of scenarios where three were chosen (Case 1, 2 and 3). These cases were chosen to represent the full range of scenarios, whereupon the one that balances energy reduction, separation performance and operational practicality, i.e., leveraging existing equipment (e.g., control valve), was chosen as the most favorable practical optimum studied.

In this study, the most beneficial and practical scenario is defined as "optimal". Balancing energy efficiency and product quality, representing a practical optimum achievable operating point rather than a mathematically guaranteed global optimum.

2.4. Side Draw Configuration. Following the optimization of the base case, the column configuration was modified by extending the number of trays and implementing a side-draw stream design to isolate and remove benzene and its precursors. This configuration is further explained in the results section and was conceptualized based on confidential internal discussions with refinery personnel, with the primary objective of enhancing total benzene removal.

After fully defining the new configuration, illustrated in Figure 3, a second simulation was run, focusing on key performance indicators such as benzene concentration in the product stream, total benzene removed and overall energy consumption.

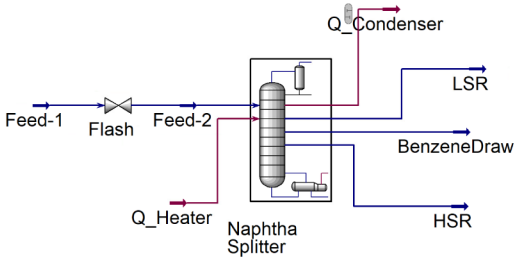

Figure 3. Naphtha splitter with benzene removal HYSYS model.

2.5. Sensitivity Analysis and Performance Benchmarking. The same sensitivity analysis methodology was applied as before by varying process conditions and column parameters independently, with a focus on maximizing benzene removal while minimizing energy consumption.

This configuration's performance was then benchmarked against the current base case model, and metrics such as benzene removal and changes in energy duty were then compared to validate if the side draw provided the desired improvements without sacrificing energy efficiency.

3. RESULTS AND DISCUSSION

3.1. The Process Feed. As summarized in Table 2, the splitter feed, whole naphtha from the hydrotreating section, enters the column at 115 °C and 160 kPa with an average volumetric flow of ≈141 m^3 h^{-1}. These values were obtained from plant DCS and laboratory data over a stable 15-day operating window, ensuring representative steady-state conditions. The simulated inlet conditions matched plant data within measurement uncertainty, confirming that the column inlet specification in Aspen HYSYS accurately reflects real operation.

Table 2. Feed Conditions of the Splitter

Plant Data	
Temperature [°C]	115
Pressure [kPa]	160
Molar Flow [kg mol/h]	Not Available
Mass Flow [kg/h]	102,017
Std Ideal Liq. Vol Flow [m^3/h]	141.1

The feed is introduced at tray 24, consistent with classical design criteria in which the feed stage is selected to approximate the point where feed composition and enthalpy most closely match the column's internal equilibrium conditions. Placing the feed near its thermal and compositional equilibrium zone minimizes internal energy imbalances and hydraulic perturbations, thereby improving stage efficiency.[17,21] Such positioning ensures that the incoming stream encounters vapor and liquid phases of similar temperature and composition, which enhances phase contacting and maintains column stability.

Upstream of the feed stage, a pressure drop from 950 to 160 kPa occurs across the control valve, producing partial flashing of

https://doi.org/10.1021/acs.iecr.5c03368
Ind. Eng. Chem. Res. 2025, 64, 23622−23637

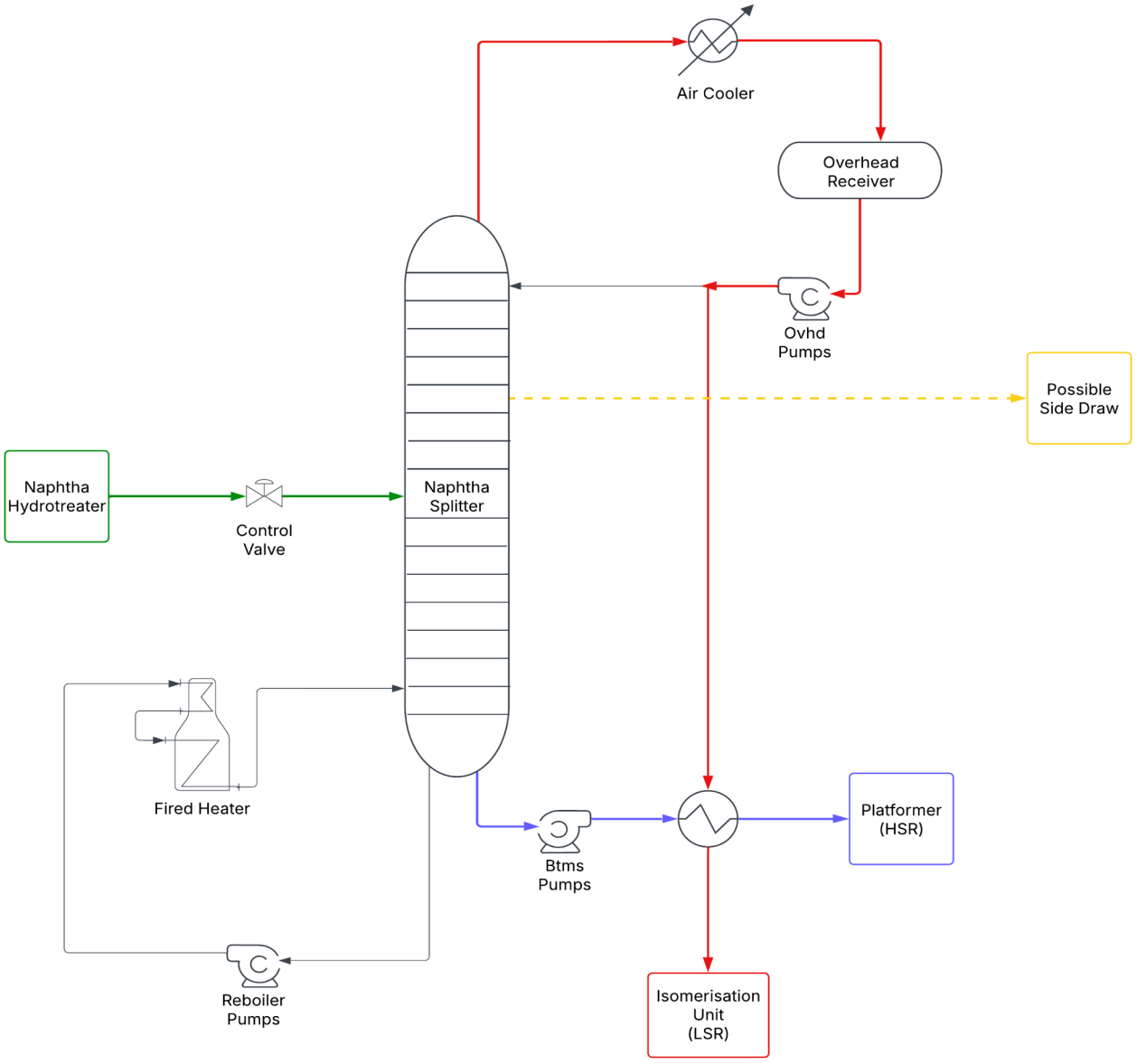

Figure 4. Process flow diagram of naphtha splitter.

the liquid feed. The isenthalpic pressure drop reduces downstream saturation; since the incoming liquid is hotter than the new saturation temperature, a portion of the liquid flashes and the feed enters the column as a two-phase mixture with a predistributed vapor fraction, effectively serving as a self-generated preheater.[22]

The enthalpy partition between liquid and vapor thus reduces the additional heat duty required in the reboiler to initiate full column vaporization, consistent with the energy-integration principles reported by Dejanović et al.[6] for hydrocarbon fractionation systems.

Maintaining a mixed-phase feed quality (≈0.1−0.3 vapor fraction) is advantageous. Too-liquid feeds increase reboiler load, whereas all-vapor feeds reduce liquid downflow and mass-transfer area efficiency. Optimal feed qualities in the 10−25% vapor range have been shown to enhance tray efficiency and lower overall energy consumption in naphtha distillation service.[17,23] Therefore, the observed feed condition corresponds closely to the recommended thermodynamic regime for high-efficiency operation (Figure 4).

From an operational perspective, the control valve serves not only as a pressure regulator but also as an energy-efficiency lever. By adjusting the valve's downstream pressure, the refinery can simultaneously influence feed vapor fraction and tray-24 flash temperature, directly coupling hydraulic control with energy optimization, a principle widely utilized in refinery column tuning.[13] This interaction between valve ΔP, feed quality, and internal vapor load establishes the physical basis for the sensitivity analyses of temperature and pressure discussed in subsequent sections.

3.2. Base Case Model. The existing, unmodified naphtha splitter operations are represented by the base case model, which was thoroughly validated in collaboration with the refinery team by adjusting tray efficiencies and parameters so that key outputs (key components' levels, process conditions, and flow rates) were as closely matching real plant data as possible.

To ensure the accuracy and completeness of the developed process model, a detailed calibration, as mentioned earlier under the methodology, was performed closely with the refinery team using real plant data. Due to data constraints, the focus of this

https://doi.org/10.1021/acs.iecr.5c03368
Ind. Eng. Chem. Res. 2025, 64, 23622−23637

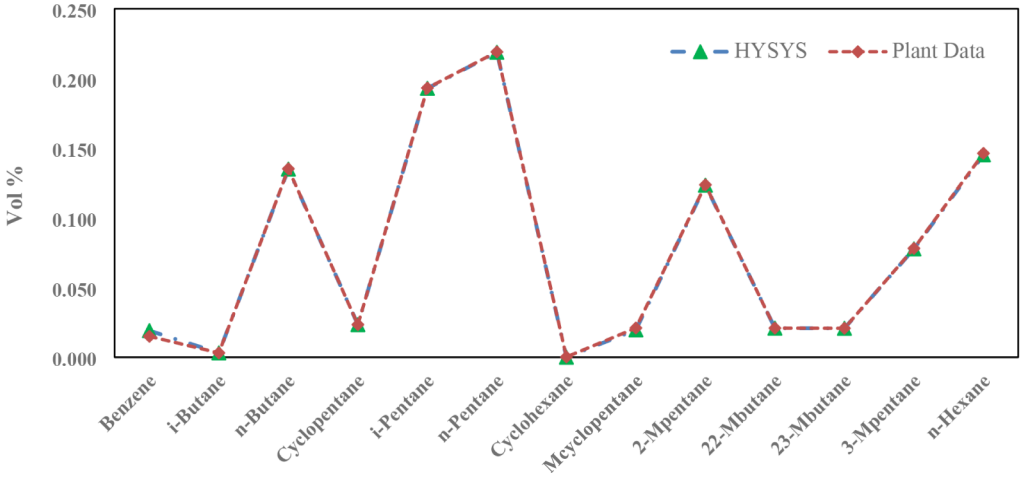

Figure 5. LSR compositions: HYSYS vs Plant Data.

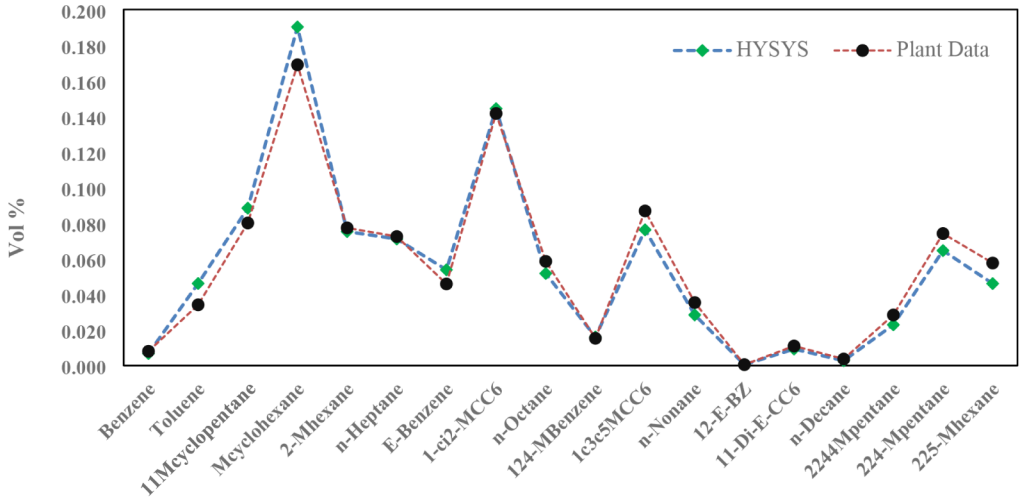

Figure 6. HSR compositions: HYSYS vs Plant Data.

validation was on comparing the light and heavy naphtha fractions, i.e., LSR and HSR, respectively, compositions obtained from Aspen HYSYS with actual measured data. Hence, the results of this comparison are shown in Figures 5 and 6 for LSR and HSR, respectively.

Model performance was validated by comparing simulated and measured product compositions for both the light-naphtha (LSR) and heavy-naphtha (HSR) cuts (Figures 5 and 6). The plotted data show close alignment between predicted and actual component profiles, confirming that the model reproduces overall cut behavior. Detailed numerical comparisons are listed in Tables 3 and 4, where individual component deviations rarely exceed 0.02 vol %.

To quantify accuracy, the mean absolute percentage deviation (MAPD) was calculated as:

$$\mathrm{MAPD} = \frac{1}{N}\sum_{i=1}^{N}\left|\frac{y_{i,\mathrm{sim}} - y_{i,\mathrm{plant}}}{y_{i,\mathrm{plant}}}\right| \times 100 \quad (1)$$

yielding 10.3% for LSR and 13.7% for HSR. Such deviations fall within accepted refinery-simulation tolerance (<15%)[19,20] and align with industry reports for equilibrium-based digital-twin models of comparable complexity.[6]

Table 3. Validation of Key LSR Compositions

Components	Plant Data LSR (% vol)	HYSYS LSR (% vol)	Deviation (%)
Benzene	0.015	0.0191	0.0041
i-Butane	0.0031	0.0031	0
n-Butane	0.1352	0.135	−0.0002
Cyclopentane	0.0234	0.0234	0
i-Pentane	0.1932	0.1929	−0.0003
n-Pentane	0.2191	0.2188	−0.0003
Cyclohexane	0.0002	0	−0.0002
Mcyclopentane	0.021	0.0197	−0.0013
2-Mpentane	0.1237	0.1235	−0.0002
22-Mbutane	0.0209	0.0209	0
23-Mbutane	0.0208	0.0208	0
3-Mpentane	0.0781	0.0778	−0.0003
n-Hexane	0.1463	0.1452	−0.0011

The trend consistency between HYSYS and plant data—particularly the dominance of *n*-pentane and *n*-hexane in LSR and of methyl cyclohexane and ethylbenzene in HSR—confirms correct relative-volatility ordering and cut separation behavior.[23] Residual differences arise mainly from sampling and chromatographic uncertainty, unmeasured heavy tails, and finite mass-transfer effects that equilibrium models idealize.[22]

https://doi.org/10.1021/acs.iecr.5c03368
Ind. Eng. Chem. Res. 2025, 64, 23622−23637

Table 4. Validation of Key HSR Compositions

Components	Plant Data HSR (vol %)	HYSYS HSR (vol %)	Deviation (%)
Benzene	0.008	0.0068	−0.0013
Toluene	0.0341	0.0461	0.012
11Mcyclopentane	0.0801	0.0884	0.0083
Mcyclohexane	0.169	0.1902	0.0212
2-Mhexane	0.0773	0.0753	−0.0021
n-Heptane	0.0725	0.0711	−0.0014
E-Benzene	0.0459	0.0538	0.0079
1-ci2-MCC6	0.1416	0.1443	0.0027
n-Octane	0.0585	0.0517	−0.0068
124-MBenzene	0.0153	0.016	0.0007
1c3c5MCC6	0.0869	0.0762	−0.0106
n-Nonane	0.0354	0.0284	−0.007
12-E-BZ	0.0005	0.0005	0
11-Di-E-CC6	0.011	0.0093	−0.0017
n-Decane	0.0037	0.0027	−0.001
2244Mpentane	0.0284	0.0229	−0.0055
224-Mpentane	0.0742	0.0646	−0.0096
225-Mhexane	0.0576	0.0461	−0.0115

Although direct condenser and reboiler duty measurements were unavailable from plant historians, the simulated condenser-to-reboiler duty ratio (∼2:1) matched the design ratio typical for naphtha splitters,[17] validating the model's overall energy balance.

Consequently, the base-case digital twin faithfully reproduces the real column's key operating signatures in both composition and energy trends. This validated model (Figures 5 and 6; Tables 3 and 4) serves as a robust foundation for the subsequent sensitivity analyses of feed temperature, pressure, and reflux ratio.

Although data on component distribution across trays was not available, it is important to note that these deviations are still very small in absolute terms, confirming that the model successfully replicates the general composition behavior of the column.

At the same time, it was not possible to obtain exact historical energy duty data for the condenser and heater, which is a clear limitation of this study; however, the primary objective of this work was to serve as a digital twin for the column, comparing its relative changes in energy usage and separation efficiency.

3.3. Sensitivity Analysis. *3.3.1. Effect of Feed Temperature.* Figure 7 shows the relationship between feed temperature and total column energy duty. Increasing the feed temperature from 110 to 140 °C markedly reduces the reboiler load, with the steepest decline (approximately 30%) observed within the first 10 °C rise to 120 °C. This behavior reflects a direct thermodynamic effect: a hotter feed enters the column with a larger vapor fraction, thereby lowering the latent-heat demand in the reboiler. In essence, a portion of the vaporization work is supplied upstream, decreasing the external heat requirement.

The condenser duty, however, remains nearly constant across this range because the overhead product composition and hence its latent-heat load change little. Similar asymmetry between reboiler and condenser responses has been reported for light-hydrocarbon distillation by Manyele[21] and Kiss,[17] confirming that energy savings from feed heating primarily accrue on the boiling side.

From a phase-equilibrium standpoint, feed preheating modifies the q-line (the fraction of liquid in the feed), thereby shifting the intersection point with the column operating lines. A higher feed temperature flattens the q-line, effectively reducing the number of ideal stages required for a given separation at constant reflux.[23] Yet beyond a certain threshold (≈120 °C in this case), additional heating yields diminishing returns because the feed approaches its bubble point and further vaporization provides little enthalpy leverage.

The compositional consequences are shown in Figure 8. With rising feed temperature, the methyl cyclopentane fraction in the light-naphtha (LSR) cut increases slightly, while *n*-hexane concentration decreases, signifying a marginal loss of separation efficiency. This outcome can be rationalized through vapor−liquid equilibrium (VLE) theory, where higher feed enthalpy elevates column temperatures, reducing the relative volatility (α) between adjacent components.

According to Raoult's law and the Clausius−Clapeyron relation, $\alpha(T) \approx \exp\left[\frac{\Delta H_{vap}}{R}\left(\frac{1}{T_2} - \frac{1}{T_1}\right)\right]$. Hence, as T rises, α decreases, promoting heavier species to migrate into lighter fractions.[22] The increased M-cyclopentane slip into the LSR is

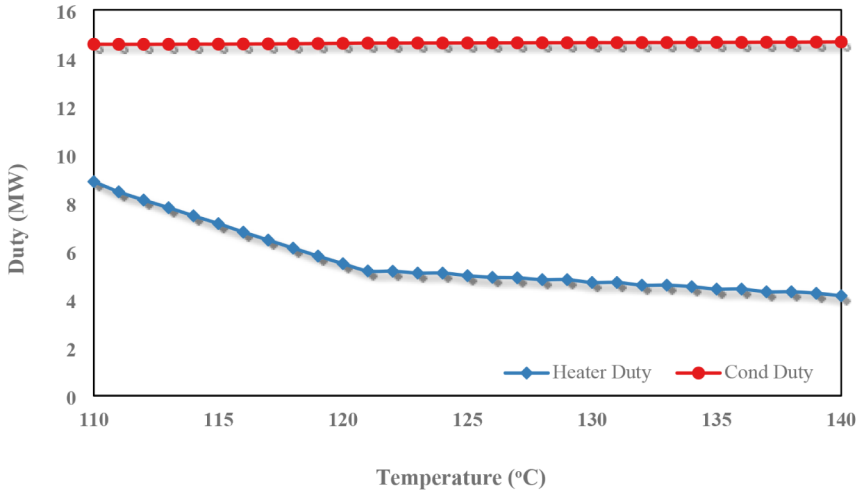

Figure 7. Effect of feed temperature on energy intensity.

https://doi.org/10.1021/acs.iecr.5c03368
Ind. Eng. Chem. Res. 2025, 64, 23622−23637

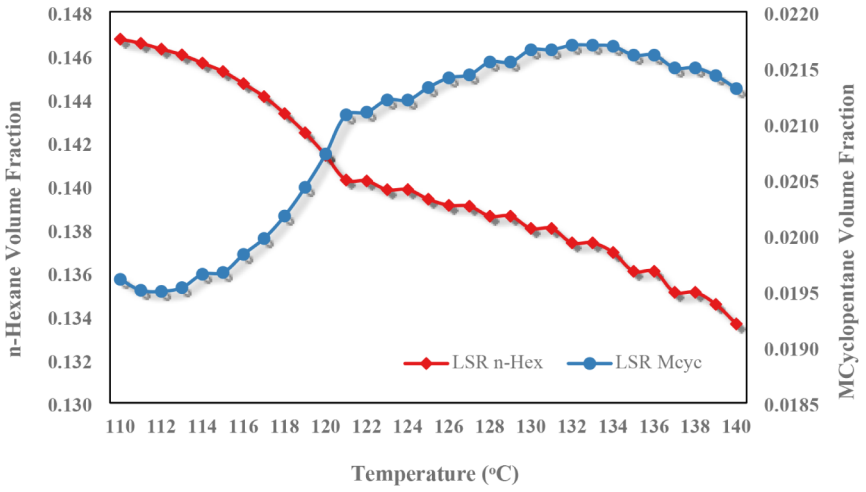

Figure 8. Effect of feed temperature on separation efficiency.

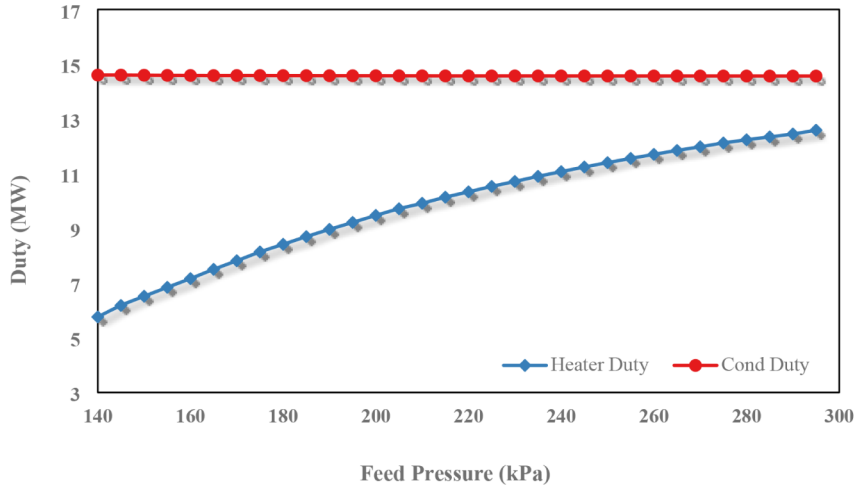

Figure 9. Effect of feed pressure on energy intensity.

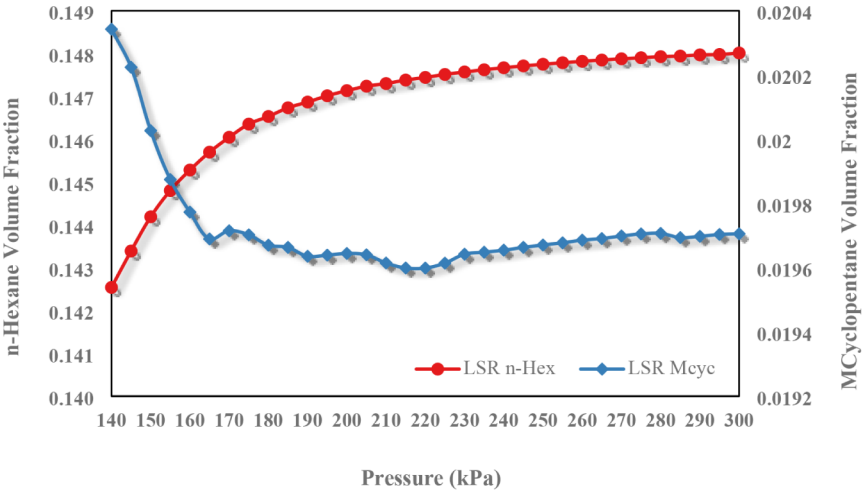

Figure 10. Effect of feed pressure on separation.

therefore a predictable consequence of reduced volatility contrast at elevated temperature.

The opposing trends in energy and selectivity define a classic trade-off curve: heating the feed saves reboiler energy but marginally degrades cut purity. Similar patterns are documented for hydrocarbon splitters by Dejanović et al.,[6] who observed that feed preheating above the optimal range weakens component discrimination despite lower utility demand. Balancing these competing effects, an operating window of 120−130 °C emerges as the most favorable region, providing near-maximum energy

https://doi.org/10.1021/acs.iecr.5c03368
Ind. Eng. Chem. Res. 2025, 64, 23622−23637

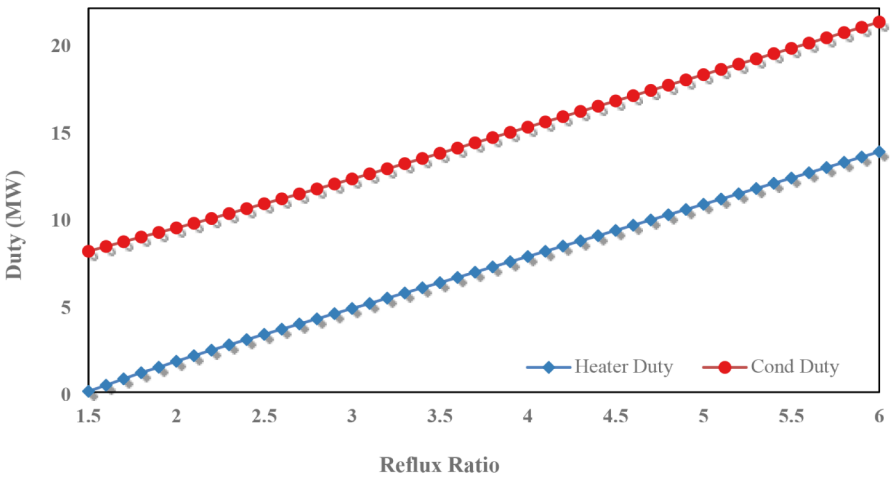

Figure 11. Effect of reflux ratio on the energy intensity.

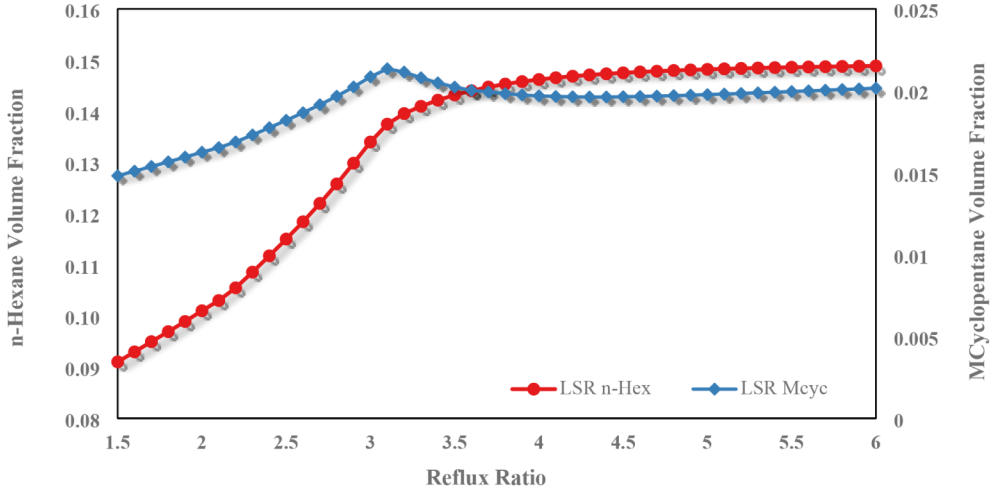

Figure 12. Effect of reflux in separation.

efficiency while maintaining acceptable LSR purity. Operation above 130 °C offers negligible additional savings and risks compromising reformer-feed quality.

3.3.2. Effect of Feed Pressure. Figure 9 illustrates that increasing the feed pressure from 140 to 300 kPa causes a monotonic rise in reboiler duty while the condenser duty remains almost constant.

This outcome follows directly from first-principles thermodynamics. At higher pressures, the liquid feed's bubble-point temperature increases, demanding more sensible heat to reach the vaporization threshold. Consequently, additional energy is required in the reboiler to generate the same vapor flow. The condenser duty is comparatively insensitive because the overhead composition, and hence the latent-heat load of condensation, changes little with moderate pressure variation.[21,23]

This behavior can be interpreted through the Clausius–Clapeyron relation,

$$\frac{dP}{dT} = \frac{\Delta H_{vap}}{T\Delta V_{vap}} \quad (2)$$

which implies that for a positive latent heat, higher P requires higher T for phase equilibrium.

Thus, at elevated column pressure, every theoretical stage must operate at a higher temperature, shifting the entire temperature profile upward and increasing the reboiler's thermal load.[22]

The corresponding effect on separation is shown in Figure 10. Only a small improvement in cut sharpness is observed at higher pressures: the LSR becomes slightly leaner in methyl cyclopentane, and *n*-hexane purity rises marginally.

As pressure rises, component vapor-pressure curves flatten, and α approaches unity.[17] Therefore, further pressurization yields diminishing separation benefit but a steep energy penalty, a classic case of thermodynamic nonlinearity in hydrocarbon distillation.[6]

From a process-systems perspective, pressure adjustment couples directly to feed enthalpy via the control valve ΔP. Increasing downstream pressure elevates both the flash temperature and the feed's liquid fraction, effectively reversing the enthalpy-saving mechanism described in Section 3.3.1.

This interaction emphasizes that pressure optimization cannot be treated independently of temperature control; both variables act through the same vapor–liquid equilibrium framework.[13]

In general, the analysis confirms that moderate pressure increases raise column energy consumption with only marginal separation improvement.

https://doi.org/10.1021/acs.iecr.5c03368
Ind. Eng. Chem. Res. 2025, 64, 23622−23637

Table 5. Key Metrics Comparison

Case	Pressure (kPa)	Temperature (°C)	Reflux Ratio	Heater Duty (MW)	Condenser Duty (MW)	Mcyclopentane (LSR) (vol %)	*n*-Hexane (LSR) (vol %)	Comments
Base	160	115	3.8	7.17	14.58	0.1970	0.1453	Reference operation
Case 1	160	125	3.3	3.5	13.19	0.0199	0.1247	Lowest energy; Slight purity loss
Case 2	220	125	3.3	5.69	13.08	0.0207	0.1410	Balanced Optimum
Case 3	200	122	3.5	6.28	13.69	0.0203	0.1432	High reflux; Rising duty

Operating below ≈240 kPa provides a practical compromise that minimizes reboiler duty, preserves adequate product purity and maintains safe mechanical margins.

These findings are consistent with refinery optimization studies showing that pressure reductions in light-naphtha distillation typically save 10−20% reboiler energy without compromising separation efficiency.[17,21] The validated digital-twin results, therefore, capture the expected thermodynamic trend and provide quantitative limits for pressure control in real-plant operation.

Based on this analysis, an operating pressure below 240 kPa is recommended, as it maximizes energy efficiency without compromising separation efficiency.

3.3.3. Effect of Reflux Ratio. Figure 11 demonstrates how varying the reflux ratio between 1.5 and 6 affects the thermal performance of the naphtha splitter.

A clear positive correlation exists between reflux and energy consumption in both the reboiler and condenser: as the reflux ratio increases, the total circulation of liquid and vapor within the column intensifies, raising the latent-heat load in both exchangers. The reboiler must generate additional vapor to sustain the higher internal flow, and the condenser must remove the corresponding heat of condensation.

This proportional relationship between reflux and total duty is a well-established characteristic of distillation systems.[24,25]

The phenomenon can be interpreted through mass-transfer and enthalpy-balance considerations. At a higher reflux ratio, the internal liquid flow rate, L, rises relative to the vapor flow, V, increasing the liquid-to-vapor ratio, L/V. This enhances component contacting and drives the composition of the distillate and bottoms closer to their equilibrium limits.

However, the additional condensation and vaporization cycles required to maintain the elevated liquid-to-vapor ratio translate directly into increased energy use in both the condenser and reboiler.[17]

The impact of reflux on separation efficiency is shown in Figure 12. At low reflux (below ≈2.5), the column exhibits poor fractionation where methyl cyclopentane slips into the LSR remains high, and *n*-hexane purity is low.

Between reflux ratios of 3 and 4, sharp improvements occur: methyl cyclopentane in the LSR decreases, and *n*-hexane concentration rises, indicating stronger component discrimination. Beyond a reflux of ≈4.5, further increases yield negligible compositional improvement, while the energy penalty continues to grow steeply.

This inflection point defines the practical optimum, where incremental reflux no longer produces proportional purity gains, a classic diminishing-return profile observed in numerous distillation studies[6,25]

Thermodynamically, this behavior arises because increasing reflux expands the internal approach to equilibrium by supplying more liquid for condensation, thereby improving mass-transfer driving forces at each tray.[23]

Once the tray compositions approach equilibrium limits, additional reflux cannot significantly alter vapor composition, so the process becomes energy-limited rather than mass-transfer-limited.

In operational terms, excessive reflux also increases column hydraulic load, raising downcomer backup and flooding risk, and imposes higher duty on the reboiler circuit, which can reduce equipment lifetime through thermal cycling.[22]

Consequently, maintaining a reflux ratio between 3 and 4 offers the best trade-off between product purity and energy efficiency for this column, consistent with industrial heuristics for naphtha fractionators.[17]

3.4. Summary of Sensitivity Analysis Outcome. The sensitivity results summarized in Table 5 integrate the separate effects of feed temperature, feed pressure, and reflux ratio on both energy consumption and product selectivity. The analysis reveals the expected but quantitatively important trade-offs among these operating variables: temperature primarily governs feed enthalpy and reboiler load, pressure affects boiling-point elevation and vapor−liquid equilibrium, and reflux ratio dictates internal mass-transfer intensity and hence separation sharpness.

3.4.1. Energy Behavior. As seen from Table 5, heater duty decreases markedly with increasing feed temperature but increases with feed pressure and reflux ratio. The most energy-efficient scenario (Case 1) is achieved at 125 °C and 160 kPa, where partial feed flashing reduces the external heat requirement by more than 50% relative to the base case. However, this condition slightly degrades light-cut purity, confirming the thermodynamic limit where further preheating lowers relative volatility.[22,23] Conversely, raising the pressure to 220 kPa (Case 2) increases absolute duty but provides better internal stability and controllability due to reduced vapor density fluctuations, a trade-off commonly exploited in refinery operations.[13] The condenser duty remains nearly constant across all cases because the overhead composition changes minimally since its energy is dominated by latent heat rather than sensible enthalpy.[21]

3.4.2. Separation Performance. The LSR composition trends show that methyl cyclopentane content decreases and *n*-hexane increases as the reflux ratio rises from 3.3 to 3.5, indicating improved light-cut quality. However, higher reflux ratios also elevate reboiler duty disproportionately, demonstrating the classical diminishing-return relationship between reflux and purity.[17,25] Increasing feed temperature above 125 °C reverses this trend by reducing α-values among C_6−C_6 hydrocarbons, which allows heavier components, such as MCP, to slip into the LSR.[6] Hence, the operating point that balances energy demand and separation efficiency corresponds to Case 2 (220 kPa, 125 °C, reflux 3.3), where both energy and compositional objectives converge.

3.4.3. Thermodynamic Rationale. At 220 kPa, the feed's equilibrium temperature (∼125 °C) aligns closely with its bubble point, ensuring partial vaporization before entry. This increases the feed's quality ($q \approx 0.25$), minimizing reboiler duty without imposing significant loss in relative volatility. The

https://doi.org/10.1021/acs.iecr.5c03368
Ind. Eng. Chem. Res. 2025, 64, 23622−23637

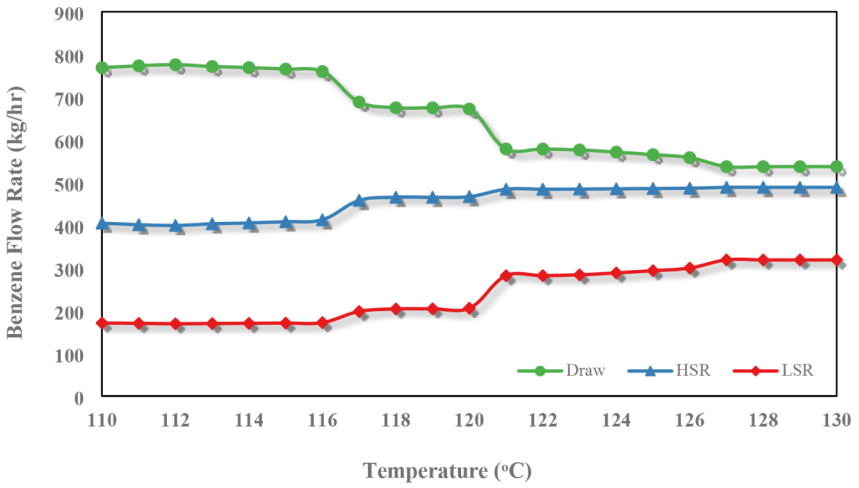

Figure 13. Effect of temperature on benzene removal.

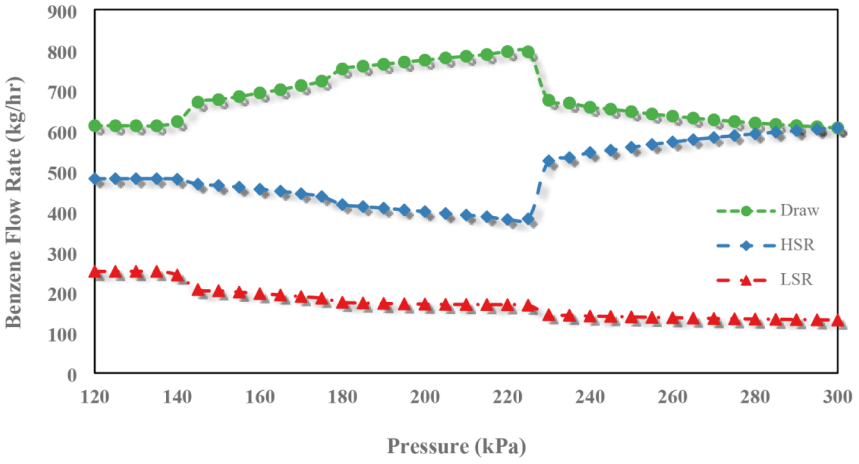

Figure 14. Effect of pressure in benzene removal.

accompanying reflux ratio of 3.3 maintains adequate internal mass transfer while avoiding excessive utility cost or hydraulic stress. These combined effects define a practical optimum, i.e., the best achievable compromise under existing equipment constraints rather than a theoretical global minimum. Such "operational optimal" is typical in industrial revamps where energy, purity, and controllability compete.[13,23]

3.5. Side Draw Configuration Performance. *3.5.1. Modifications vs Original Design.* The most substantial change to the column is the introduction of a benzene side draw, positioned at tray 49 (see Figure 4), which was absent in the original configuration.

The location was selected using simulated composition profiles to coincide with the point of maximum benzene liquid concentration along the column, which is roughly the interface between the light-naphtha (C_5−C_6) and heavy-naphtha (C_6−C_6) fractions. At this tray, benzene exhibits an intermediate volatility: it is more volatile than most C_7^+ components but less than C_6 paraffins, enabling selective withdrawal without disrupting either product end.[17,23]

Introducing a midcolumn draw exploits the equal-composition principle of side streams: the liquid composition at the draw tray equals that of the tray's bulk liquid, so removal efficiency is determined primarily by draw location.[22] This design allows benzene and its precursors, principally methyl cyclopentane and cyclohexane, to be extracted before they distribute into both end products. Selective removal of these intermediates upstream of the reformer mitigates later benzene formation via dehydrogenation, thereby improving compliance with Clean Fuels II standards.[10,14]

To maintain adequate theoretical stages after the side draw, the column was extended by several trays above and below the draw point, preserving overall rectifying and stripping-section balance. This adjustment prevents loss of product-cut sharpness and compensates for the reduction in internal liquid traffic caused by the draw.[6] The modification requires only internal replacement (no shell extension), making it a low-CAPEX revamp achievable during a standard maintenance turnaround.

3.5.2. Effect of Feed Temperature. The influence of feed temperature on benzene removal performance is presented in Figure 13. As feed temperature increases from 110 to 130 °C, the total benzene removed via the side draw initially rises, reaches a maximum near 120 °C, and then declines. The temperature dependence arises from competing vapor−liquid equilibrium effects that govern benzene distribution among the column sections.

At lower feed temperatures, benzene's vapor pressure (and hence volatility) is reduced relative to lighter paraffins. According to Raoult's law and Antoine correlations, benzene's partial pressure increases exponentially with temperature;[15,26]

https://doi.org/10.1021/acs.iecr.5c03368
Ind. Eng. Chem. Res. 2025, 64, 23622−23637

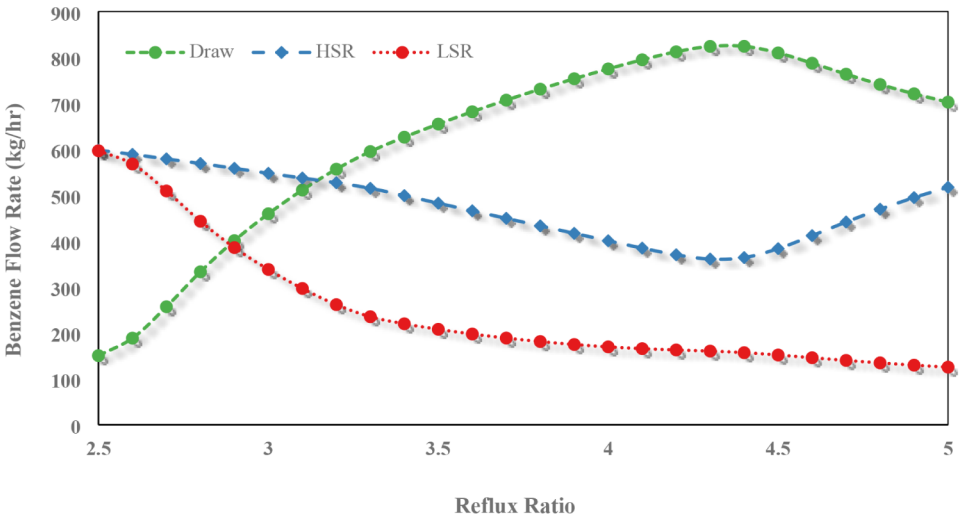

Figure 15. Effect of reflux in benzene removal.

therefore, cooler operation favors benzene condensation into the liquid phase near its dew-point region. The side draw, sampling liquid from tray 49, thus captures a higher benzene fraction under moderately cooler conditions.

As temperature increases beyond ∼120 °C, the equilibrium shifts toward the vapor phase: more benzene migrates upward with the lighter fraction, reducing its concentration at the draw tray. This explains the decline in removal efficiency at higher temperatures.[21,22]

Simultaneously, the HSR benzene flow decreases while the LSR benzene flow rises, indicating a redistribution rather than a net accumulation. This observation is consistent with benzene's intermediate volatility (boiling point ≈ 80.1 °C) and agrees with literature reports showing that modest temperature reductions around the midcolumn zone enhance aromatic extraction in light-naphtha service.[10]

Thermodynamically, the sensitivity can be interpreted through relative-volatility shifts. The benzene−*n*-hexane system exhibits an $\alpha \approx 2.1$ at 120 °C, decreasing with further heating due to reduced $\frac{\Delta H_{vap}}{T^2}$ dependence in the Clausius−Clapeyron equation.[23] Hence, operating near 120 °C optimizes the volatility gap between benzene and its neighboring paraffins, maximizing selective removal while minimizing energy penalty.

From an operational viewpoint, the cooler feed conditions marginally increase reboiler duty but enhance benzene capture efficiency. Therefore, the optimal feed-temperature window (115−125 °C) represents a pragmatic compromise between energy savings and regulatory performance. Maintaining feed within this range ensures that the side draw consistently removes 500−600 kg h^{-1} of benzene-rich liquid while keeping total column energy consumption within the optimized limits established in Section 3.4.

3.5.3. Effect of Feed Pressure. The effect of feed pressure on benzene extraction is shown in Figure 14. As column pressure increases from 120 to 230 kPa, the benzene removal rate via the side draw initially improves, reaches a maximum around 230 kPa, and then declines. This nonlinear trend results from opposing thermodynamic mechanisms that control vapor−liquid equilibrium (VLE) in multicomponent hydrocarbon systems.

At moderate pressures (<230 kPa), raising pressure elevates the liquid density and decreases vapor-phase molar volume, thereby enhancing mass transfer between phases and favoring benzene retention in the liquid.

According to the Clausius−Clapeyron relation, the slope,

$$\frac{dP}{dT} = \frac{\Delta H_{vap}}{T \Delta V_{vap}} \tag{3}$$

indicates that higher pressure raises the boiling point of each component, shifting the equilibrium toward the condensed phase.

Because benzene has a lower vapor pressure than paraffins of similar carbon number, this shift selectively increases its liquid-phase concentration at the side-draw tray.[22,23]

Consequently, total benzene recovery rises with pressure up to ≈230 kPa. Beyond this optimum, the benefits reverse as further pressurization compresses the VLE curves, reducing relative volatility (α) among C_6−C_6 hydrocarbons and flattening the composition gradient across stages.[17]

When $\alpha \rightarrow 1$, the driving force for benzene−paraffin separation diminishes, allowing benzene to revaporize and migrate upward into the LSR product.

Additionally, higher column temperatures associated with increased pressure promote partial thermal degradation of separation efficiency, since benzene's volatility increases more slowly with T than that of lighter paraffins, leading to vapor-phase enrichment rather than liquid capture.[21]

This behavior is also observed experimentally in refinery simulations of catalytic-cracking gasoline, where intermediate-boiling aromatics display maximum recovery within a limited pressure window before redistribution between overhead and bottoms.[10] In this study, operating above ≈230 kPa caused a 10−15% decline in benzene flow through the side draw, confirming the predicted VLE crossover point.

From a process-control standpoint, feed pressure is not only a thermodynamic parameter but also a manipulated variable governed by the control-valve set-point upstream of the column. Adjusting this pressure simultaneously alters feed-flash temperature and vapor fraction (Section 3.3.2), creating a coupled interaction between feed enthalpy and benzene equilibrium.

Maintaining pressure in the range 200−230 kPa ensures stable vapor load, sufficient benzene condensation in the midsection, and manageable reboiler duty. Operating beyond this window

https://doi.org/10.1021/acs.iecr.5c03368
Ind. Eng. Chem. Res. 2025, 64, 23622−23637

Table 6. Key Metrics Comparison—Benzene Removal

Case	Pressure (kPa)	Temperature (°C)	Reflux Ratio	Heater Duty (MW)	Condenser Duty (MW)	Benzene Flow (HSR) (kg/h)	Benzene Flow (LSR) (kg/h)	Benzene Draw (kg/h)	Comments
Optimized (Baseline)	220	125	3.3	5.69	13.08	417.6	927.6	0	No side draw; Reference case.
Benzene Removal	220	125	3.3	2.32	9.75	517.9	257.8	569.5	Moderate draw; Balanced performance
Benzene Removal+	190	120	3.8	3.67	10.97	430.1	213.6	701.5	Maximum benzene removal; Slightly higher energy

would impose higher energy costs and compromise product compliance without further improving benzene removal.

3.5.4. Effect of Reflux Ratio. The influence of the reflux ratio on benzene extraction is depicted in Figure 15. As the reflux ratio increases from 2.5 to 5, the total benzene flow through the side draw initially rises, reaches a maximum between 3.5 and 4.5, and then declines. This nonmonotonic trend originates from the competing effects of enhanced liquid−vapor contacting and altered internal hydraulics within the column.

At low reflux ratios (<3), the internal liquid flow is insufficient to achieve full vapor condensation on each tray, resulting in limited benzene condensation in the midcolumn region.

Because benzene has intermediate volatility, inadequate reflux allows a significant portion to ascend with lighter paraffins into the LSR cut, reducing its concentration at the side-draw stage.

Increasing the reflux ratio intensifies internal circulation and raises the L/V ratio, improving counter-current contact and promoting condensation of aromatic species such as benzene on intermediate trays.[23]

Consequently, benzene removal efficiency increases sharply up to the optimal range. Beyond a reflux ratio of ≈4.5, however, the benefits reverse, as excessive reflux generates higher internal liquid holdup and downcomer back-pressure, which reduces vapor residence time and enhances entrainment and remixing effects.[22]

The resulting hydraulic imbalance drives partial revaporization of benzene and increases its recirculation between the draw tray and neighboring stages. This causes a net decline in removal despite higher overall liquid flow, a phenomenon also observed by Dejanović et al.[6] and Kiss[17] for multicomponent hydrocarbon columns.

Thermodynamically, benzene's response to reflux variation is linked to its relative volatility ($\alpha \approx 2-2.5$ at midcolumn temperatures) and to the enthalpy-composition (H-x) profile of the liquid phase.

Increasing reflux cools the upper column section, decreasing vapor-phase benzene concentration and shifting its equilibrium distribution downward toward the draw tray.[21]

Once the column temperature gradient stabilizes, further reflux only increases energy use, with marginal additional condensation because the system approaches local equilibrium.[17]

From an energy standpoint, each increment in reflux increases both reboiler and condenser duties almost linearly, since more liquid must be vaporized and subsequently condensed per cycle.

Therefore, operating near the 3.5−4.0 range provides the best compromise, maximizing benzene removal while keeping energy intensity within the bounds established by the earlier operational optimization (Section 3.4). Reflux ratios beyond ≈4.5 yield negligible purity gains but impose substantial penalties in steam and cooling-water consumption.

3.6. Summary of Sensitivity Analysis Outcome. The combined results of the side-draw sensitivity analysis are presented in Table 6, which compares three representative scenarios: the previously optimized baseline (Case 2 from Section 3.4), the Benzene Removal case, and a Benzene Removal + case that prioritizes maximum aromatic extraction. The variables evaluated were feed temperature, feed pressure, and reflux ratio, each adjusted within feasible operational limits to determine their combined effect on benzene removal, energy consumption, and stream distribution.

3.6.1. Energy and Separation Performance. Introducing the side draw substantially lowered total column duties while enabling selective aromatic extraction. Relative to the base case, the Benzene Removal configuration reduced total reboiler and condenser energy by ≈33%, while the Benzene Removal + case achieved slightly lower overall savings (≈28%) but higher benzene capture (Table 6).

These differences stem from the higher reflux ratio (3.8) and lower operating pressure (190 kPa) adopted in Benzene Removal + , which intensified mass transfer but partially offset energy gains due to increased liquid circulation. Such energy−purity trade-offs are typical in multicomponent side-draw systems.[17,23]

This analysis confirms that feed temperature, pressure, and reflux ratio are critical variables influencing benzene removal performance with the new side-draw configuration. With this in mind, Table 6 presents a comparison between the proposed design, the base case model, the optimized model, and a new case focusing primarily on benzene removal, while maintaining the previously defined constraints and philosophies.

The side draw diverts a benzene-rich liquid stream (∼0.5−0.7 t h^{-1}) from the column midpoint, preventing its distribution into both light and heavy products.

In the Benzene Removal case, benzene in the LSR product decreased by ∼72%, while total column energy demand fell by one-third.

These simultaneous improvements indicate that energy efficiency and aromatic control are not mutually exclusive when side-draw placement and operating conditions are co-optimized. This conclusion is consistent with the process-intensification findings of Dejanović et al.[6] and Wang et al.[10]

3.6.2. Thermodynamic Interpretation. The integrated results reveal three distinct control mechanisms:

Feed temperature modifies the equilibrium vapor fraction entering the column. Moderate heating (∼120 °C) increases vapor load enough to stabilize the temperature profile and favor benzene condensation near the side-draw tray, while excessive heating (>125 °C) lowers relative volatility and shifts benzene into the vapor phase.[22]

Feed pressure governs the volatility contrast between benzene and paraffins. Operating around 220 kPa

https://doi.org/10.1021/acs.iecr.5c03368
Ind. Eng. Chem. Res. 2025, 64, 23622−23637

Table 7. Optimal Operating Point

	Pressure (kPa)	Temperature (°C)	Reflux	Heater Duty (MW)	Condenser Duty (MW)	Mcyclopentane (LSR) (vol %)	*n*-Hexane (LSR) (vol %)
Case 2	220	125	3.3	5.69	13.08	0.0207	0.141

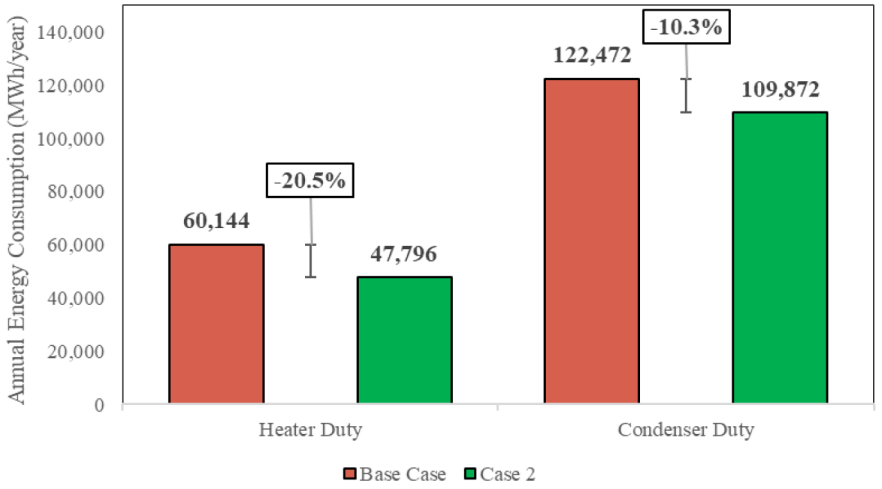

Figure 16. Base case vs optimized energy intensity.

maximizes benzene's liquid-phase retention without suppressing mass-transfer efficiency. Beyond 230 kPa, α-values among C_6-C_6 species converge, reducing selectivity and increasing reboiler duty.[17,21] Reflux ratio determines the local liquid-to-vapor ratio (L/V) around the draw tray. A ratio of 3.5−4.0 provides sufficient liquid to strip benzene from the rising vapor while avoiding entrainment losses or excessive utility load.[25] Together, these interactions define a multivariable optimum where feed $T \approx 120-125$ °C, feed $p \approx 210-225$ kPa, and reflux ≈ 3.5.

Within this envelope, the column operates near the thermodynamic "sweet spot" that minimizes reboiler duty while achieving maximum benzene removal efficiency.

3.6.3. Operational and Economic Implications. Because the side draw and tray adjustments are confined to the internal structure, the modification constitutes a low-CAPEX retrofit: no shell replacement or new external exchangers are required.

The only additional hardware involves draw nozzles, internal retray, and piping tie-ins, all implementable during a normal turnaround period.

This configuration thus offers a cost-effective pathway to achieve benzene-spec compliance and energy decarbonization simultaneously.

Moreover, the newly validated operating window serves as the baseline for the economic and CO_2 analysis in Section 4.

4. DISCUSSION AND IMPLICATIONS OF SENSITIVITY ANALYSIS

4.1. Base Case Optimal Point. The sensitivity analysis revealed strong interdependence among process variables—particularly temperature, pressure, and reflux ratio—which all significantly impact energy consumption and separation efficiency. Case 2, shown in Table 7, was selected as the optimal operating point due to its balance between energy savings and product purity.

By adjusting the pressure drop across the existing control valve to raise feed pressure to 220 kPa, the feed temperature correspondingly increases to 125 °C due to vapor−liquid equilibrium effects. This adjustment leverages the existing control valve, meaning no new equipment is required, and thus there is no capital expenditure. This proves to be an efficient solution since it effectively eliminates the need for external preheating, which would incur increased capital and operating costs for the possible new heat exchanger and increased steam demand. In addition to this, the significant reduction in energy duties will potentially extend the reboiler and condenser's service life and reduce maintenance frequency due to lower thermal stress. Moreover, operating at higher pressures will also typically promote overall reliability in its operations, therefore making this scenario adequate for long-term operations.

This increase in both pressure and temperature also stabilizes the column, which counteracts the lower reflux ratio (3.3), aligning with the thermodynamic principles where increased pressure typically raises boiling points.[22]

As demonstrated in Figure 16, Case 2 offers significant energy savings, more specifically, a 20.5% heater duty reduction and 10.3% condenser duty reduction, while maintaining product quality.

4.2. Effectiveness of the Side Draw Configuration. Following the first phase of the analysis and optimization, the focus turned to targeting benzene extraction while balancing the savings we made earlier.

The added side draw effectively extracts benzene as expected from intermediate stages by redistributing lighter components, which is in line with other studies around aromatic precursor recovery.[10] As depicted in Table 8 and Figures 17 and 18, the side draw achieves a 42% reduction in total benzene in the product stream. A further optimized case (Benzene Removal +) delivers a 52% reduction while lowering energy consumption by 33% compared to the base case.

Similar to the base optimization, the side-draw efficacy depends on controlling the operating conditions (temperature, pressure, and reflux), where the existing control valve again plays a critical role in the dynamic adjustment of the feed pressure and therefore the temperature. This again reduces the reliance on

https://doi.org/10.1021/acs.iecr.5c03368
Ind. Eng. Chem. Res. 2025, 64, 23622−23637

Table 8. Optimal Operating Point—Benzene Removal

	Benzene Removal	Benzene Removal +
Pressure (kPa)	220	190
Temperature (°C)	125	120
Reflux	3.3	3.8
Heater Duty (MW)	2.32	3.67
Cond Duty (MW)	9.75	10.97
Benzene Flow (HSR) (kg/h)	517.9	430.1
Benzene Flow (LSR) (kg/h)	257.8	213.6
Benzene Flow (Removal) (kg/h)	569.5	701.5

external utilities or new equipment, which lowers overall costs. Detailed cost and payback data for the side-draw configuration cannot be disclosed due to refinery confidentiality. However, this modification involves primarily adjustments to column internals and control optimizations rather than large-scale additions.

In addition to the removal of benzene, it is critical to remove components which would later be converted into benzene in the catalytic reforming unit; these components are methyl cyclopentane and cyclohexane.[14]

4.3. Economic Evaluation. The energy-efficiency improvements identified in both the operationally optimized and side-draw configurations translate directly into substantial financial and environmental benefits. The analysis uses a representative industrial blended energy tariff of R 2.35 kWh^{-1}[27] and 320 operating days yr^{-1}, as provided by the host refinery. Because the condenser and reboiler account for >90% of the total thermal duty, energy savings in these components dominate the economic balance.

4.3.1. Energy Cost Savings. For Case 2 (operational optimization), the combined heater- and condenser-duty reduction of ≈14% corresponds to ≈11 520 MWh yr^{-1} of energy saved.

At the stated tariff, this equates to an annual cost reduction of ≈ZAR 27 million (USD 1.45 million).

For the Benzene Removal + configuration, the 33% total energy reduction yields ≈27 700 MWh yr^{-1} of savings, equivalent to ZAR 65 million (USD 3.5 million yr^{-1}).

These values are summarized in Tables 9 and 10 and confirm that even modest operating adjustments can generate multi-million-dollar savings at no or minimal capital cost.

Comparable revamp studies in refinery distillation columns report similar magnitudes of benefit, typically achieving payback periods below 6 months.[6,17]

4.3.2. Carbon-Emissions Impact. Because South Africa's power grid is primarily coal-based, the country's average emission factor of 0.96 t CO_2e MWh^{-1}[28] was used to estimate avoided emissions.

Thus:

- 14% reduction (11 520 MWh yr^{-1}) → ≈11 060 t CO_2 yr^{-1} avoided.
- 33% reduction (27 725 MWh yr^{-1}) → ≈26 620 t CO_2 yr^{-1} avoided.

At the current carbon-tax rate of R 236 t^{-1} CO_2e,[29] these savings correspond to ≈ZAR 2.6 million (USD 0.15 million) and ZAR 6.3 million (USD 0.35 million) yr^{-1}, respectively.

When combined with direct energy savings, the total annual economic benefit of the side-draw revamp exceeds ZAR 71.44 million yr^{-1} (USD 3.8 million), underscoring the financial relevance of energy−emission co-optimization.

4.3.3. Sensitivity to Energy Inflation. Electricity tariffs in South Africa have risen by >190% since 2014 and are projected to increase by ≈12% yr^{-1}.[30]

Applying a conservative 5% escalation rate yields a 10-year cumulative saving of ≈ZAR 898.6 million (USD 52.6 million) with no discounting for the side-draw case. This highlights the robustness of the revamp even under moderate cost-growth assumptions.

4.3.4. CAPEX and Payback. The retrofit involves only internal modifications such as additional trays, a single side-draw nozzle, and minor piping. Based on analogous refinery projects, total installed cost is expected to remain <2% of the unit's annual maintenance budget, or approximately USD 0.1−0.2 million.

Given the projected annual savings (>USD 3 million), the simple payback period is <1 month, rendering the investment economically compelling. This magnitude of return is consistent with industrial case studies of thermally coupled or dividing-wall retrofits reported by Kiss[17] and Gorak and Sorensen.[23]

4.3.5. Strategic Implications. Beyond direct cost savings, the energy and emissions reductions improve the refinery's competitiveness under tightening carbon-tax and fuel-spec regimes.

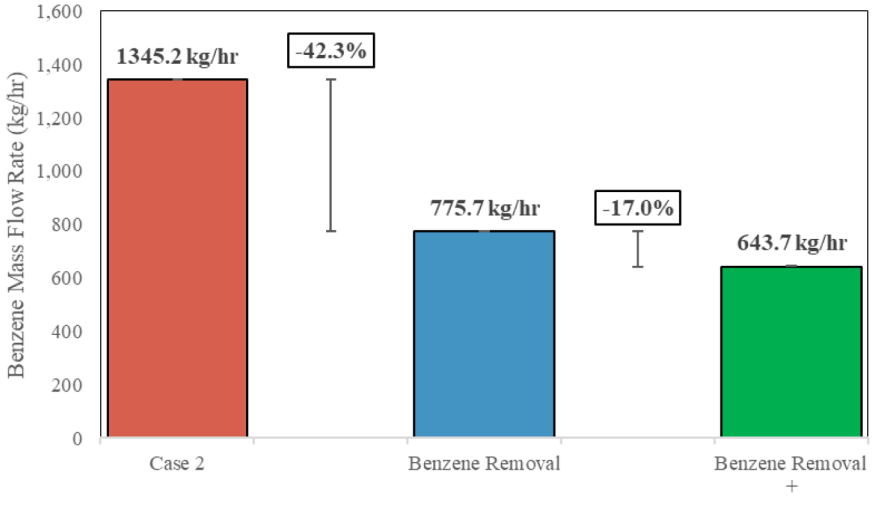

Figure 17. Total benzene breakthrough.

https://doi.org/10.1021/acs.iecr.5c03368
Ind. Eng. Chem. Res. 2025, 64, 23622−23637

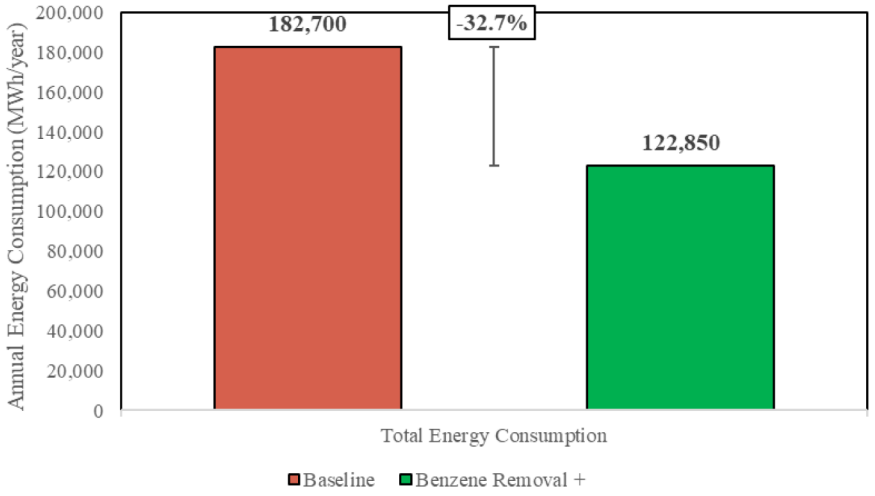

Figure 18. Base case vs optimized side draw.

Table 9. 14% Energy Reduction from Case 2

	Case 2
Energy Savings (MWh/year)	11,520
Cost Savings	ZAR 27,072,000 (~USD 1,448,592)

Table 10. 33% Energy Reduction from Benzene Removal Case

	Benzene Removal +
Energy Savings (MWh/year)	27,725
Cost Savings	ZAR 65,153,750 (~USD 3,486,279)

By meeting the Clean Fuels II benzene limit preemptively and lowering CO_2 intensity, the plant strengthens its eligibility for future carbon-credit or sustainability-linked financing.

The results exemplify how digital-twin-guided low-CAPEX optimization can achieve measurable decarbonization without major process overhauls; a strategy directly aligned with global refinery-efficiency benchmarks.[5]

5. CONCLUSIONS

This study demonstrates that a refinery naphtha splitter can achieve simultaneous energy reduction and benzene-spec compliance through combined operational optimization and a low-CAPEX structural revamp guided by a validated digital twin.

The systematic variation of feed temperature, pressure, and reflux ratio identified an optimum at 220 kPa, 125 °C, reflux 3.3. This condition exploits the pressure−enthalpy coupling across the existing control valve to generate partial feed flashing, achieving a 14% reduction in total energy duty (≈11 520 MWh yr^{-1}) and ≈US $1.4 million yr^{-1} cost saving without any hardware modification.

After the first phase, the installation of a midcolumn side draw at tray 49, combined with minor tray rearrangements, enabled selective removal of benzene and its precursors. The optimized configuration produced a total energy reduction of ≈33% (27 700 MWh yr^{-1}) and a 52% decrease in benzene content across product streams. The retrofit requires only internal modifications implementable during a turnaround and therefore constitutes a low-CAPEX (<2% of annual maintenance) solution.

The results confirm that partial-flash feed conditioning, moderate column pressurization, and midcolumn withdrawal create a thermodynamically synergistic regime where energy, purity, and controllability improve concurrently. The study provides quantitative evidence that operational and structural optimization need not be mutually exclusive, a principle applicable to other energy-intensive separation units in petroleum and chemical manufacturing.

Although the present model assumes steady-state operation, future research should integrate dynamic simulation and model-predictive control (MPC) to evaluate transient behavior and automatic set-point adjustment. Extending the digital-twin framework to other columns or process trains could further enhance plant-wide decarbonization strategies.

■ ASSOCIATED CONTENT

Supporting Information

The Supporting Information is available free of charge at https://pubs.acs.org/doi/10.1021/acs.iecr.5c03368.

Naphtha splitter HYSYS workbooks (PDF)

■ AUTHOR INFORMATION

Corresponding Author

Nejat Rahmanian − *Chemical Engineering Program, School of Computing and Engineering, Faculty of Management, Sciences, and Engineering., University of Bradford, Bradford BD7 1DP, U.K.*; Email: n.rahmanian@bradford.ac.uk

Authors

Pedro Dias − *Chemical Engineering Program, School of Computing and Engineering, Faculty of Management, Sciences, and Engineering., University of Bradford, Bradford BD7 1DP, U.K.*; orcid.org/0009-0007-5348-9056

Abbas Rajaei − *Chemical Engineering Program, School of Computing and Engineering, Faculty of Management, Sciences, and Engineering., University of Bradford, Bradford BD7 1DP, U.K.*

Complete contact information is available at: https://pubs.acs.org/10.1021/acs.iecr.5c03368

Notes

The authors declare no competing financial interest.

https://doi.org/10.1021/acs.iecr.5c03368
Ind. Eng. Chem. Res. 2025, 64, 23622−23637

■ ACKNOWLEDGMENTS

The authors would like to take a moment to thank the refinery team for their incredible support, as this work simply would not have been possible without them.

■ REFERENCES

(1) U.S. Energy Information AdministrationCountry Analysis Brief: South Africa*The U.S. Energy Information Administration.*; U.S. Energy Information Administration, 2024.
(2) Surinder, P. *Refining Processes Handbook*; Elsevier, 2003.
(3) SGS. South Africa Delays New Fuel Specifications to July 2027. 2022. https://inspire.sgs.com/content/100103337/south-africa-delays-new-fuel-specifications-to-july-2027 (accessed September 2025).
(4) S&P Global Commodity Insights. South Africa Deferring Tighter Fuel Specs Could Prop Up Refineries. July 12, 2022.https://www.spglobal.com/commodity-insights/en/news-research/latest-news/chemicals/071222-south-africa-deferring-tighter-fuel-specs-could-prop-up-refineries (accessed September 2025).
(5) Worrell, E.; Galitsky, C.; Masanet, E. Energy Efficiency Improvement and Cost Saving Opportunities for Petroleum Refineries: An ENERGY STAR Guide for Energy and Plant Managers. *U.S. Environmental Protection Agency*, 2015. https://www.energystar.gov/sites/default/files/tools/ENERGY_STAR_Guide_Petroleum_Refineries_20150330.pdf (accessed September 2025).
(6) Dejanović, I.; Matijašević, L.; Olujić, Ž. Dividing Wall Columns in Chemical Process Industry: A Review on Current Activities. *Chem. Eng. Process* **2010**, *49* (6), 559−580.
(7) CEP; Optimize Naphtha Processing Using Dividing-Wall Technology*CEP Magazine*; 2021.https://www.aiche-cep.com/cepmagazine/august_2021/MobilePagedArticle.action?articleId=1711654 (accessed September 2025)
(8) Chemical Processing. Energy Saver: Dividing Wall Columns Supercharge Distillation Efficiency. *Chemical Processing (online), May 2023*. https://www.chemicalprocessing.com/voices/energy-saver/article/55260619/energy-saver-dividing-wall-columns-supercharge-distillation-efficiency (accessed September 2025).
(9) Pappas, I.; Bindlish, R.; Ali, M.; Pistikopoulos, E.N. Optimal Operation of an Industrial Dividing Wall Column. *Ind. Eng. Chem. Res.* **2023**, *62* (37), 13960−13974.
(10) Wang, Z.; Ke, M.; Song, Z.; Li, J.; Sun, J. Benzene Reduction Process Simulation and Optimization in Catalytic Cracking Gasoline Distillation. *Processes* **2023**, *11* (1), 151.
(11) Osman, W. S.; Fadel, A. E.; Salem, S. M.; Shoaib, A. M.; Gadallah, A. G.; Bhran, A. A. Optimum Design of Naphtha Recycle Isomerization Unit with Modification by Adding De-Isopentanizer. *Processes* **2023**, *11* (12), 3406.
(12) Lee, J. Y.; Kim, Y. H.; Hwang, K. S. Application of a Fully Thermally Coupled Distillation Column for Fractionation Process in Naphtha Reforming Plant. *Chem. Eng. Process.* **2004**, *43* (4), 495−501.
(13) Robbins, L. *Distillation Control, Optimization, and Tuning: Fundamentals and Strategies*; CRC Press, 2011. DOI: .
(14) Donaldson, H.Platforming−Reactions of Pure Hydrocarbons. In*Paper presented at the 3rd World Petroleum Congress*; One petro:the Netherlands, 1951, p.WPC−4321.
(15) Goodwin, R. D. Benzene Thermodynamical Properties from 279 to 900 K. *J. Phys. Chem. Ref. Data* **1988**, *17* (4), 1541−1636.
(16) Søreide, I.; Whitson, C. H. Peng-Robinson Predictions for Hydrocarbons, CO2, N2, and H2 S with Pure Water and NaCI Brine. *Fluid Phase Equilib.* **1992**, *77*, 217−240.
(17) Kiss, A. A. *Advanced Distillation Technologies: Design, Control and Applications*; John Wiley & Sons, 2013.
(18) Hussain, M. S.; Fares, M. N.; Taher, M. A. Optimization and Design of a New Column Sequencing for Crude Oil Distillation at Basrah Refinery. *Open Eng.* **2024**, *14* (1), 20220571.
(19) Rahmanian, N.; Ilias, I. B.; Nasrifar, K. Process Simulation and Assessment of a Back-up Condensate Stabilization Unit. *J. Nat. Gas Sci. Eng.* **2015**, *26*, 730−736.
(20) Rahmanian, N.; Bt Jusoh, L. S.; Homayoonfard, M.; Nasrifar, K.; Moshfeghian, M. Simulation and Optimization of a Condensate Stabilisation Process. *J. Nat. Gas Sci. Eng.* **2016**, *32*, 453−464.
(21) Manyele, S.V. Analysis of the Effect of Feed Composition and Thermal Conditions on Distillation Plant Performance Using a Computer Model. *J.Chem. Eng. Mater.Sci.* **2021**, *12* (2), 40−63.
(22) Green, D. W.; Southard, M. Z. *Perry's Chemical Engineers' Handbook*, 9th ed.; McGraw Hill Professional, 2018.
(23) Gorak, A.; Sorensen, E. *Distillation: fundamentals and Principles*; Academic Press, 2014.
(24) Almalike, A. S.; Almalike, L. B.; Ali, A. A.; Al-Asadi, A. A.; Al-Matwari, M. A. Simulation and Energy Saving Optimization in Naphtha Splitter. *Int. Trans. J.Eng.gement.appl.Sci.Technol.* **2021**, *12*, 1−10.
(25) Fitriah, F.; Sari, D. A. Optimization of Distillation Column Reflux Ratio for Distillate Purity and Process Energy Requirements. *Int.J.Basic Appl. Sci.* **2023**, *12* (2), 72−81.
(26) NIST. *Benzene Properties*, NIST, 2025.
(27) NERSA. *South Africa Electricity Tariff Report*; NERSA, 2024.
(28) South African Government. *South Africa's 2022 Grid Emission Factors Report*. South African Government, 2024.
(29) South African Government. *Carbon Tax Act 15 of 2019*; South African Government, 2019.
(30) Eskom FY 2026 Tariffs. *Distribution*. https://www.eskom.co.za/distribution/2025-2026-price-increase/ (accessed 28 March 2025).

https://doi.org/10.1021/acs.iecr.5c03368
Ind. Eng. Chem. Res. 2025, 64, 23622−23637